Astrophysics studies relevant to stellar x-ray bursts

J. J. He, J. Hu, L. Y. Zhang, S. W. Xu, A. Parikh, H. Yamaguchi, D. Kahl, P. Ma, S. Z. Chen, J. Su, Y. Wakabayashi, Y. Togano, S. Hayakawa, H. W. Wang, W. D. Tian, R. F. Chen, B. Guo, T. Nakao, T. Teranishi, J. Y. Moon, H. S. Jung, T. Hashimoto, A. A. Chen, D. Irvine, K. I. Hahn, N. Iwasa, T. Yamada, T. Komatsubara, C. S. Lee, and S. Kubono

Citation: AIP Conference Proceedings **1594**, 176 (2014); doi: 10.1063/1.4874064
View online: http://dx.doi.org/10.1063/1.4874064
View Table of Contents: http://scitation.aip.org/content/aip/proceeding/aipcp/1594?ver=pdfcov
Published by the AIP Publishing

Astrophysics Studies Relevant to Stellar X-Ray Bursts

J.J. He[*], J. Hu[*], L.Y. Zhang[*], S.W. Xu[*], A. Parikh[†,**], H. Yamaguchi[‡], D. Kahl[‡], P. Ma[*], S.Z. Chen[*], J. Su[§], Y. Wakabayashi[¶], Y. Togano[¶], S. Hayakawa[‡], H.W. Wang[‖], W.D. Tian[‖], R.F. Chen[*], B. Guo[§], T. Nakao[‡], T. Teranishi[††], J.Y. Moon[‡‡], H.S. Jung[‡‡], T. Hashimoto[§§], A.A. Chen[¶¶], D. Irvine[¶¶], K.I. Hahn[***], N. Iwasa[†††], T. Yamada[†††], T. Komatsubara[‡‡‡], C.S. Lee[‡‡] and S. Kubono[*,¶]

[*]*Institute of Modern Physics (IMP), Chinese Academy of Sciences (CAS), Lanzhou 730000, China*
[†]*EUETIB, Universitat Politècnica de Catalunya, Barcelona E-08036, Spain*
[**]*Institut d'Estudis Espacials de Catalunya, Barcelona E-08034, Spain*
[‡]*CNS, the University of Tokyo, Wako Branch at RIKEN, 2-1 Hirosawa, Wako, Saitama 351-0198, Japan*
[§]*China Institute of Atomic Energy (CIAE), P.O. Box 275(46), Beijing 102413, China*
[¶]*RIKEN Nishina Center, 2-1 Hirosawa, Wako, Saitama 351-0198, Japan*
[‖]*Shanghai Institute of Applied Physics (SINAP), Chinese Academy of Sciences (CAS), Shanghai 201800, China*
[††]*Department of Physics, Kyushu University, 6-10-1 Hakozaki, Fukuoka 812-8581, Japan*
[‡‡]*Department of Physics, Chung-Ang University, Seoul 156-756, Republic of Korea*
[§§]*RCNP, Osaka University, 10-1 Mihogaoka, Ibaraki, Osaka, 567-0047, Japan*
[¶¶]*Department of Physics & Astronomy, McMaster University, Hamilton, Ontario L8S 4M1, Canada*
[***]*Department of Science Education, Ewha Womans University, Seoul 120-750, Republic of Korea*
[†††]*Department of Physics, University of Tohoku, Miyagi 980-8578, Japan*
[‡‡‡]*Department of Physics, University of Tsukuba, Ibaraki 305-8571, Japan*

Abstract. Two reactions of $^{14}O(\alpha,p)^{17}F$ and $^{18}Ne(\alpha,p)^{21}Na$ provide the pathways for breakout from the hot CNO cycles to the rp-process in type I X-ray bursts. To better determine their astrophysical reaction rates, resonance parameters of the compound nuclei ^{18}Ne and ^{22}Mg have been investigated by the resonant elastic scattering of $^{17}F+p$ and $^{21}Na+p$, respectively. The ^{17}F and ^{21}Na radioactive ion beams were produced at the CNS Radioactive Ion Beam Separator and impinged on the thick proton targets. The excitation functions were obtained with a thick-target method over a wide excitation energy range. The resonance parameters in the compound nuclei ^{18}Ne and ^{22}Mg have been determined through an *R*-matrix analysis. New reaction rates of these two (α,p) reactions are recalculated. The astrophysical impact for the $^{18}Ne(\alpha,p)^{21}Na$ reaction has been investigated through one-zone postprocessing X-ray burst calculations.

Keywords: Reaction induced by unstable nuclei, Decay by proton emission, nuclear astrophysics
PACS: 25.40.Ny, 25.40.Cm, 21.10.HW, 26.50.+x, 26.30.Ca

INTRODUCTION

Type I X-ray bursts (XRBs), one of the most fascinating astrophysical phenomena, are characterized by sudden dramatic increases in luminosity of roughly 10–100 s in duration, with a total energy release of about 10^{39} erg per burst. These recurrent phenomena (on timescales of hours to days) have been the subject of many observational, theoretical and experimental studies (for reviews see *e.g.*, [1, 2, 3]). The characteristics of XRBs have been surveyed extensively in a number of space-borne X-ray satellite observatory missions, including RXTE, BeppoSAX, Chandra, HETE-2, and XMM/Newton. More than 90 galactic XRBs have been identified since their initial discovery in 1976. These observations have provided abundant data and opened a new era in X-ray astronomy. The bursts have been interpreted as being generated by thermonuclear runaway on the surface of a neutron star that accretes H- and He-rich material from a less evolved companion star in a close binary system [4, 5]. The accreted material burns stably through the hot, β-limited carbon-nitrogen-oxygen (HCNO) [6, 7] cycles, giving rise to the persistent flux. Once critical temperatures and densities are achieved, breakout from this region can occur through, *e.g.*, α-induced reactions on the waiting point nuclei ^{14}O, ^{15}O and ^{18}Ne. Through the rapid proton capture process (rp-process) [8, 9, 10], this eventually results in a rapid increase in energy generation (ultimately leading to the XRB) and nucleosynthesis up to A$\sim$100 mass region [11, 12]. Among the possible breakout reactions, breakout may occur through the $^{14}O(\alpha,p)^{17}F$ and

Origin of Matter and Evolution of Galaxies 2013
AIP Conf. Proc. 1594, 176-183 (2014); doi: 10.1063/1.4874064

^{18}Ne(α,p)^{21}Na reactions [13]; however, the actual astrophysical conditions under which these reaction occur depend critically on the actual ^{14}O(α,p)^{17}F and ^{18}Ne(α,p)^{21}Na thermonuclear rates.

Contributions from the resonant states dominate the ^{14}O(α,p)^{17}F reaction rate, and therefore the resonant parameters for the excited states above the α threshold (Q_α=5.115 MeV [14]) in the compound nucleus ^{18}Ne are required. So far, although our understanding of the reaction rate of ^{14}O(α,p)^{17}F has been greatly improved via, *e.g.*, indirect studies [15, 16, 17, 18, 19, 20, 21, 22], direct study [23], as well as time-reversal studies [24, 25, 26], most of the required parameters (such as, J^π and Γ_α) have still not been sufficiently well determined over stellar temperatures achieved in XRBs (≈0.2–2 GK). In the temperature region below ∼1 GK, a state at E_x=6.15 MeV (tentatively assigned as 1^-, see below) is thought to dominate the ^{14}O(α,p)^{17}F rate [15]. About twenty-five years ago, Wiescher *et al.* [27] predicted a J^π=1^- state at E_x=6.125 MeV in ^{18}Ne with a width of Γ=Γ_p=51 keV based on a Thomas-Ehrman shift calculation. Later on, Hahn *et al.* [15] observed a state at E_x=6.15±0.02 MeV through studies of the ^{16}O(^{3}He,n)^{18}Ne and ^{12}C(^{12}C,^{6}He)^{18}Ne reactions. The transferred angular momentum was restricted to be $\ell\leq$2 from their measured (^{3}He,n) angular distribution. Based on the Coulomb-shift calculation and prediction of Wiescher *et al.*, a J^π=1^- was tentatively assigned to this state. Gómez *et al.* [18] studied the resonances in ^{18}Ne by using the elastic scattering of ^{17}F+p and fitted the 6.15-MeV state with 1^- by an *R*-matrix analysis of the excitation function. However, their 1^- assignment was questioned in a later *R*-matrix reanalysis [28]. He *et al.* [28] thought that this 1^- resonance should behave as a dip-like structure (rather than the peak observed in Ref. [18]) in the excitation function due to the interference. Unfortunately, a recent low-statistics measurement could not resolve this state [22]. Recently, Bardayan *et al.* [29] reanalyzed the unpublished elastic-scattering data in Ref. [19] and also found the expected dip-like structure, however, the statistics were not sufficient to constrain the parameters of such a resonance. Therefore, it is very much necessary to determine the spin-parity of this key state on a firm experimental ground.

The reaction rate for ^{18}Ne(α,p)^{21}Na is dominated by contributions from resonances in the compound nucleus ^{22}Mg above the α threshold at 8.142 MeV [14]. The temperature region of interest in XRBs is about 0.4–2.0 GK, corresponding to an excitation region of E_x=8.6–11.0 MeV in ^{22}Mg. Previously, the α-unbound states in ^{22}Mg were extensively studied by many transfer reaction experiments [30, 31, 32, 33], and finally the uncertainty (in excitation energies of ^{22}Mg) of about 1–15 keV was achieved for most states above the α threshold [33]. With these precise energies, the uncertainties in ^{18}Ne(α,p)^{21}Na rate were largely reduced. These indirect studies mainly focused on the determination of excitation energies, and the spin-parity assignments were not strictly constrained. Some spin-parity assignments were made [30, 33, 34] simply by referring to those of mirror states in ^{22}Ne; such assignments are dubious due to the high level-density in this excitation energy region. Two tentative spin-parity assignments were made in a previous low statistics measurement [35, 36] of resonant ^{21}Na+p elastic scattering, which still need to be confirmed by a high statistics experiment. So far, there are still many resonances (above the α threshold) without firm spin-parity assignments, which need to be determined experimentally. Furthermore, only two direct measurements [37, 38] for the ^{18}Ne(α,p)^{21}Na reaction have been performed. The lowest energies achieved in these studies ($E_{c.m.}$=2.0 and 1.7 MeV) are still too high compared with the energy region $E_{c.m.}\leq$1.5 MeV of interest for HCNO breakout in XRBs. New results [39] have recently become available at the ISAC II facility at TRIUMF, where the ^{18}Ne(α,p)^{21}Na cross section was determined in the energy region of $E_{c.m.}$=1.19–2.57 MeV by measuring the time-reversal reaction ^{21}Na(p,α)^{18}Ne in inverse kinematics. Nonetheless, these results are still insufficient for a reliable rate at all temperatures encountered within XRBs.

In our work, the ^{14}O(α,p)^{17}F and ^{18}Ne(α,p)^{21}Na rates are determined via the measurements of the resonant elastic scattering of ^{17}F+p and ^{21}Na+p, respectively. With this approach, the excitation functions were obtained in a wide range of 0.6–2.3 MeV in ^{18}Ne and 5.5–9.2 MeV in ^{22}Mg with the well-established thick-target method [40, 41, 42], which proved to be an effective technique in the previous studies [36, 43, 44, 45, 46]. By fitting our data with the *R*-matrix code, we have experimentally determined the J^π values for those states above the α threshold in ^{18}Ne and ^{22}Mg, respectively.

EXPERIMENTS

Both experiments were performed using the CNS Radioactive Ion Beam separator (CRIB) [47, 48], installed by the Center for Nuclear Study (CNS), the University of Tokyo, in the RI Beam Factory of RIKEN Nishina Center. The primary beams were accelerated by an AVF cyclotron (K=70) of RIKEN. The energy calibration for the Si detectors was carried out by using secondary proton beams produced with CRIB and a standard triple-α source. Two experiments are described in the following sections, respectively.

Setup for ^{17}F+p measurement

Some details about this experiment were reported elsewhere [49]. The $^{16}O^{6+}$ primary beam was accelerated up to 6.6 MeV/nucleon, and delivered to CRIB with an average intensity of 560 enA. It was impinged on a liquid-nitrogen-cooled D_2 gas target ($\sim$90 K) [50] where ^{17}F RI beam was produced via the $^{16}O(d,n)^{17}F$ reaction in inverse kinematics. The D_2 gas at 120 Torr pressure was confined in a 80-mm long cell with two 2.5 μm thick Havar foils. The ^{17}F beam was subsequently separated by the CRIB, with a purity of about 98% after the Wien-filter. At the final focal plane, the RIBs were impinged on a thick H_2 gas target, where the energy of ^{17}F beam was 61.9$\pm$0.5 MeV (measured by a silicon detector), with an average intensity of 2.5×10^5 pps. All the beams were stopped completely in this target. Here, the H_2 gas target at a pressure of 600 Torr was housed in a 300-mm-radius semi-cylindrical shape chamber sealed with a 2.5-μm-thick Havar foil as an entrance window and a 25-μm-thick aluminized Mylar foil as an exit window. Comparing to the widely-used solid CH_2 target, the gas target is free from intrinsic background from carbon. The contribution of background was evaluated through a separate run with Ar gas at 120 Torr in the target chamber.

The recoiling light particles were measured by using three ΔE-E Si telescopes at average angles of $\theta_{lab}\approx3^\circ$, 10° and 18°, respectively. In the *c.m.* frame of elastic scattering, the corresponding scattering angles are $\theta_{c.m.}\approx155^\circ\pm18^\circ$, $138^\circ\pm22^\circ$ and $120^\circ\pm22^\circ$, respectively. At $\theta_{lab}\approx3^\circ$, the telescope consisted of a 65-μm-thick double-sided-strip (16×16 strips) silicon detector and two 1500-μm-thick pad detectors. The last pad detector was used to veto any energetic light ions produced in the production target and satisfying the $B\rho$ selection, possibly not rejected entirely by the Wien filter because of scattering in the inner wall of the beam line. The configuration of the other two telescopes is similar to that at $\theta_{lab}\approx3^\circ$, except for the absence of the third veto layer.

Setup for ^{21}Na+p measurement

Some details about this experiment were reported elsewhere [51]. An 8.2 MeV/nucleon primary beam of $^{20}Ne^{8+}$ was impinged on a liquid nitrogen-cooled D_2 gas target (90 K) [50] with an average intensity of 65 pnA. The thickness of D_2 gas was about 2.9 mg/cm^2 at 530 Torr pressure. The ^{21}Na beam was produced via the $^{20}Ne(d,n)^{21}Na$ reaction in inverse kinematics. After the Wien filter, a purity of 70% for the ^{21}Na beam was achieved on the target. The beam impinged on an 8.8 mg/cm^2 polyethylene $(CH_2)_n$ target, which was thick enough to stop all the beam ions. The targets were bombarded with the ^{21}Na beam at energy about 89.4 MeV (ΔE=1.9 MeV in FWHM). The averaged beam intensity was about 2×10^5 pps. In addition, a 10 mg/cm^2 thick carbon target was used for evaluating the C background contribution.

The recoiling light particles were detected with three silicon ΔE-E telescopes centered at angles of $\theta_{Si}=0^\circ$, +14° and -14° with respect to the beam line, respectively. Each ΔE-E telescope subtended an opening angle of about 10° with a solid angle of about 27 msr in the laboratory frame. In the *c.m.* frame for elastic scattering, the relevant averaged scattering angles are determined to be $\theta_{c.m.}\approx175^\circ$ (Set 1), 152° (Set 2) and 151° (Set 3), respectively.

Identification of beam and recoiling particles

In these two experiments, two PPACs (Parallel Plate Avalanche Counters) [52] provided the timing and two-dimensional position information of the beam particles. The beam profile on the secondary target was monitored by the PPACs during the data acquisition. The beam particles were clearly identified event-by-event by the time of flight (TOF) between PPACa and the production target using the phase of RF signal provided by the cyclotron.

As for the ΔE-E telescope, the double-sided-strip (16×16 strips) ΔE detectors measured the energy, position and timing signals of the particles, and the pad E detectors measured their residual energies. This allowed for the clear identification of recoiling light particles in these two experiments.

RESULTS

The excitation functions of ^{17}F+p and ^{21}Na+p resonant elastic scattering have been reconstructed using the procedure described previously [22, 36, 42, 45]. The cross-section data were corrected for the stopping cross sections of ions in the target [42, 53].

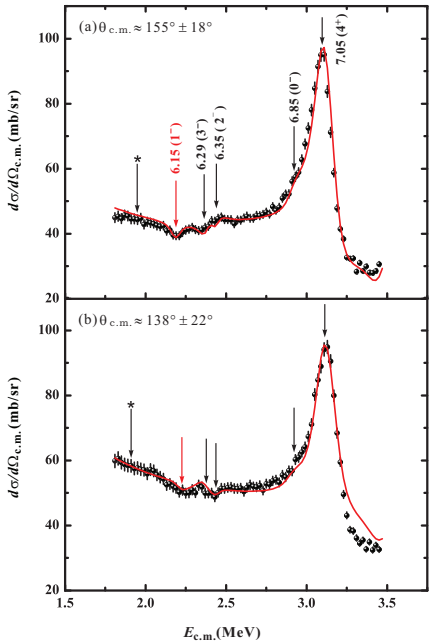

FIGURE 1. (Color online) The center-of-mass differential cross-sections for elastically scattered protons of ^{17}F+p at angles of (a)$\theta_{c.m.}\approx 155^\circ\pm 18^\circ$, and (b)$\theta_{c.m.}\approx 138^\circ\pm 22^\circ$. The background contributions (from the Ar gas run) were subtracted accordingly. The (red) curved lines represent the best overall R-matrix fits. The locations of inelastic scattering events for the 6.15-MeV state are indicated as the asterisks.

The ^{17}F+p case

The ^{17}F+p elastic-scattering excitation functions at two scattering angles are shown in Fig. 1. The normalized background spectra (taken from the Ar gas run) were subtracted accordingly. Several resonant structures were clearly observed in the spectra. In order to determine the resonant parameters of observed resonances, multichannel R-matrix calculations [54, 55, 56] (see examples [28, 57]) that include the energies, widths, spins, angular momenta, and interference sign for each candidate resonance have been performed in the present work. A channel radius of R_n=1.25×(1+17$^{\frac{1}{3}}$)≈4.46 fm appropriate for the ^{17}F+p system [15, 18, 22, 27, 28, 58] has been utilized in the calculation. The choice of radius only has minor effect on the large uncertainties quoted both for the excitation energies and widths. The ground-state spin-parity configurations of ^{17}F and proton are $5/2^+$ and $1/2^+$, respectively. Thus, there are two channel spins in the elastic channel, *i.e.*, s=2 and 3. In the present R-matrix calculation, the α partial widths (Γ_α) are neglected relative to the proton widths ($\Gamma_\alpha \ll \Gamma_p$) [15, 26]. Five resonances, at E_x=6.15, 6.28, 6.35, 6.85, and 7.05 MeV, have been analyzed, and the best overall fitting curves are shown in Fig. 1. Additionally, in order to fit the data around $E_{c.m.}$=3.2 MeV, it was necessary to include an additional known resonance ($E_x\sim$7.40 MeV, $J^\pi=2^+$, Γ_p=40 keV) [22, 26, 59] in the calculations.

According to the R-matrix analysis, a dip-like structure around $E_{c.m.}$=2.21 MeV, corresponding to the 6.15-MeV state in ^{18}Ne, is best fit as a natural-parity 1^- state (ℓ=1, s=2, Γ_p=50±15 keV) (see Fig. 1). Considering the inelastic branch, this width should correspond to the total width Γ, and agrees with Γ=53.7±2.6 keV reported before [29]. The resonance shape of this state agrees with that of the low-statistics experiment by Bardayan *et al.* [29]. The natural-parity character of state was also verified by the previous direct ^{14}O(α,p)^{17}F experiment [23]. In addition, the 3^- assignment is very unlikely, and also because of the large inelastic branch observed for this state; the unnatural-parity 2^- assignment is also unlikely based on the discussions of the 2p-emission from this state [18, 60]. Therefore, we confirmed the 1^- assignment of the important 6.15-MeV state. Our resonance shape is entirely different from the bump-like shape observed in Ref. [18]. This may be due to issues in the data as well as the R-matrix analysis (see the lower panel of Fig. 2 in Ref. [18]). As a result, J^π assignments suggested in Ref. [28] are also questionable.

In addition, it is very interesting that a shoulder-like structure around $E_{c.m.}$=2.93 MeV was observed by both

telescopes as shown in Fig. 1. This is possibly a new state at E_x=6.85±0.10 MeV. Both J^π=0$^-$ or 0$^+$ resonances can reproduce the observed shape, and here a 0$^-$ fit is shown in Fig. 1. Because of the small energy shift for the negative-parity states in this excitation energy region [59], such a state is possibly the analog state of ^{18}O at E_x=6.880 MeV (0$^-$) [61]. In fact, Wiescher *et al.* [27] predicted a J^π=0$^-$ state in ^{18}Ne, analog to the 6.88 MeV state in ^{18}O, at 6.85 MeV with a proton spectroscopic factor of C^2S_p=0.01. However, other possibilities still exist, which need to be confirmed in further data analysis.

The ^{21}Na+p case

The ^{21}Na+p elastic-scattering excitation functions at three scattering angles are shown in Fig. 2. Where the data within the dead-layer region (between ΔE and E detectors) were removed from the figure. The normalized proton yield with the C target, whose spectrum was flat and smooth as a function of energy, was less than about 1/5 of that with the $(CH_2)_n$ target. In Fig. 2, the carbon-induced background was subtracted accordingly and the uncertainties shown are mainly of statistical origin.

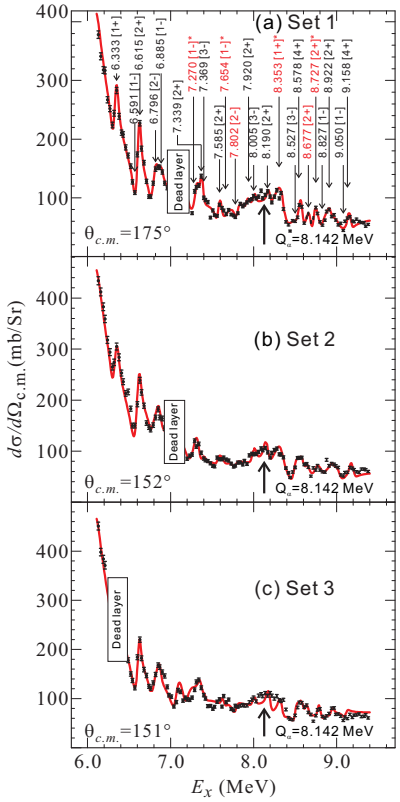

FIGURE 2. (Color online) The *c.m.* differential cross sections for the resonant elastic scattering of ^{21}Na+p measured by three sets of telescopes at different angles. The most probable *R*-matrix fitting results are shown. The data within the dead-layer region (between ΔE and E detectors) were removed. See text for details.

The excitation energies indicated on Fig. 2 are calculated by E_x=E_R+Q_p. Here, the resonance energy E_R is determined by an *R*-matrix analysis (see below), and a proton separation energy of Q_p=5.504 MeV is adopted [14]. With this thick-target technique, the $E_{c.m.}$ energy uncertainty is approximately ±(30–50) keV for those states above the α threshold based on a Monte-Carlo simulation [35, 36]. The present excitation energies agree with those adopted in Ref. [33] within the uncertainties [51].

The ^{21}Na+p excitation function has been analyzed by a multichannel *R*-matrix [54] code MULTI [58]. An overall *R*-matrix fit is also shown in Fig. 2. A channel radius of R_n=1.35(1+21$^{\frac{1}{3}}$) fm [30, 34] was adopted in the calculation. The successful reproduction of the well-known states [33, 62] at 6.333, 6.591, 6.615, and 6.796 MeV by the code (see

Fig. 2) provides confidence in the present method. In this paper, we focus on determining the resonance parameters of those states above the α threshold in ^{22}Mg, which eventually determine the ^{18}Ne(α,p)^{21}Na reaction rate.

In total, ten resonances above the α-threshold were observed and analyzed by the *R*-matrix code. For the first time, we have experimentally confirmed the J^π values tentatively assigned by Matic *et al.* [33] for seven states at 8.181, 8.519, 8.574, 8.783, 8.932, 9.080 and 9.157 MeV, and assigned here new J^π values for three states at 8.385, 8.657 and 8.743 MeV. The presently observed 8.578 MeV state is closest to the 8.574 MeV in the work of Matic *et al.* in which it was assigned to be a 4^+ state based on a shell-model calculation. Here, both 2^+ and 4^+ can fit our data very well, and hence our data support the previous 4^+ assignment. The observed 8.353 MeV state is regarded as the 8.385 MeV state of Matic *et al.* whose J^π was suggested to be 2^+ by referring to the mirror state in ^{22}Ne. In addition, we assigned it J^π=(1^+–3^+) in a previous low statistics experiment [35, 36] where 1^+ was also the most probable assignment. In this work, J^π=1^+ is again the best candidate. Furthermore, this state was only weakly populated in the previous transfer-reaction experiments [30, 32, 33] which preferentially populated the natural-parity states in ^{22}Mg. This again supports our assignment of 1^+ unnatural-parity to this state. The observed 8.677 MeV state corresponds to the 8.657 MeV state of Matic *et al.*, which was assigned as a J^π=0^+ also based on a shell-model calculation. However, such a prediction is questionable because of the high level density at such a high excitation energy region. Matic *et al.* regarded this state as the 8.613 MeV state observed in Ref. [30] where it was assumed to be 3^- by simply shifting the energy of mirror 8.741 MeV state in ^{22}Ne by ~130 keV. In this work, we assign J^π=2^+ to this state. The observed 8.727 MeV state is regarded as the 8.743 MeV state of Matic *et al.*, which was simply assumed to be the mirror of the 8.976 MeV, 4^+ state in ^{22}Ne. The present *R*-matrix fit strongly prefers a 2^+ rather than a 4^+. It is worth mentioning that our data at the scattering angle of $\theta_{c.m.}\approx152^\circ$ also support the J^π assignments discussed above.

ASTROPHYSICAL IMPLICATIONS

The astrophysical implications are still under evaluation with a revised ^{14}O(α,p)^{17}F reaction rate. Here, we only report the astrophysical implications for the newly calculated ^{18}Ne(α,p)^{21}Na rate. We have calculated the ^{18}Ne(α,p)^{21}Na rate using a narrow resonance formalism [30, 33], by using present new J^π assignments in combination with the available resonance parameters. Comparing to the most recent rate of Matic *et al.*, the present rate is much smaller below 0.13 GK. This is due to a unnatural-parity 1^+ newly assigned to the 8.385 MeV state which does not contribute to the rate anymore. As well, the present rate is about 2.1 times larger around 0.2 GK, because of our new 2^+ assignments for the 8.657 and 8.743 MeV states. Finally, the present rate is about 1.6 times larger around 1.0 GK, because of the experimental information we have adopted for the 9.542 and 10.085 MeV states as discussed above. Comparing to the other available rates, our new rate is about a factor of 2–1000 times larger within the temperature region of interest for XRBs. In addition, our new rate is about 4–10 times larger than the Hauser-Feshbach statistical-model calculation [63] beyond 0.2 GK.

The impact of our new ^{18}Ne(α,p)^{21}Na rate was examined within the framework of one-zone XRB postprocessing calculations. Different XRB thermodynamic histories were employed, including the K04 (T_{peak}=1.4 GK) and S01 (T_{peak}=1.9 GK) models from Refs. [64, 65]. For each of these histories, separate postprocessing calculations were performed using the present ^{18}Ne(α,p)^{21}Na rate and previous rates [30, 33, 34, 36, 66]; rates of all other reactions in the network [64] were left unchanged.

The rate of the ^{18}Ne(α,p)^{21}Na reaction clearly affects predictions from our models. For example, as shown in Fig. 3, a striking difference in the nuclear energy generation rate at early times (between 0.3 and 0.4 s, or equivalently, between 0.6 GK and 0.9 GK during the burst) is seen when comparing XRB calculations using the present, Chae *et al.* and Görres *et al.* rates with the K04 model. Not only does the peak energy generation rate increase by a factor of 1.4–1.8 with the present rate, but the profiles of the curves around the maxima are also rather different. We also note a change in the ^{18}Ne(α,p)^{21}Na reaction flux at these early times. For example, at 0.35 s, this reaction flux increases by a factor of 2–3 with our new rate. This contributes to the depletion of ^{15}O and ^{18}Ne at early times by a factor of 3–4 relative to abundances calculated using the Chae *et al.* [66] or Görres *et al.* [34] rates.

We note that for both the K04 and S01 models, rates from Refs. [30, 34, 36] give lower peak nuclear energy generation rates than that from Chae *et al.*, by about 10–30 %. Furthermore, the rate of Matic *et al.* gives rather similar results to those using the present rate. In particular, the calculated nuclear energy generation rates agree overall to about 5%. This is of interest: despite the different J^π values adopted in the present and Matic *et al.* ^{18}Ne(α,p)^{21}Na rate calculations (and the consequent differences in deduced thermonuclear rates - see Fig. 3), our models give very similar XRB nuclear energy generation rates. This suggests that J^π values for relevant states in ^{22}Mg are, for the moment,

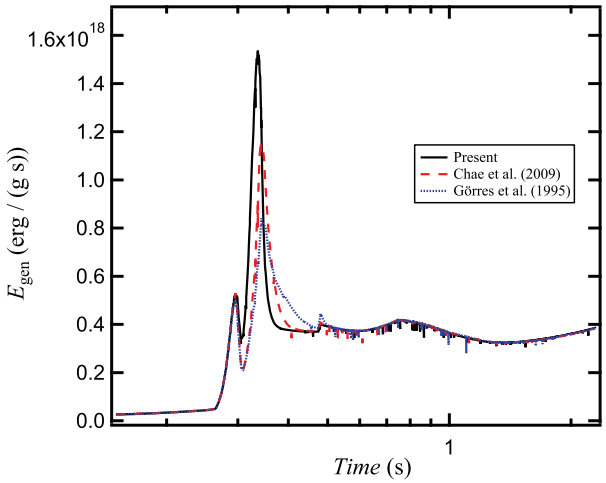

FIGURE 3. (Color online) Nuclear energy generation rates during one-zone XRB calculations using the K04 thermodynamic history [64]. Results using the present ^{18}Ne(α,p)^{21}Na rate (black solid line), the Chae *et al.* 2009 [66] rate (red dashed line) and the Görres *et al.* 1995 [34] rate (blue dotted line) are indicated.

sufficiently well known for our models. Future measurements should primarily focus on measuring other quantities of interest (such as spectroscopic factors, partial widths or the precise direct cross-section data), which can further constrain this rate. Further tests using full hydrodynamic XRB models are needed to examine these effects in detail.

ACKNOWLEDGMENTS

We would like to thank the RIKEN and CNS staff for their friendly operation of the AVF cyclotron. This work was financially supported by the National Natural Science Foundation of China (Nos. 11135005), the Major State Basic Research Development Program of China (2013CB834406), as well as the JSPS KAKENHI (No. 25800125). AP was supported by the Spanish MICINN (Nos. AYA2010-15685, EUI2009-04167), the E.U. FEDER funds as well as the ESF EUROCORES Program EuroGENESIS. A.A.C and D.I were supported by the National Science and Engineering Research Council of Canada. K.I.H was supported by the NRF grant funded by the Korea government (MSIP) (No. NRF-2012M7A1A2055625), J.Y.M, H.S.J and C.S.L by the Priority Centers Research Program in Korea (2009-0093817).

REFERENCES

1. W. Lewin, et al., *Space Sci. Rev.* **62**, 223 (1993).
2. T. Strohmayer, L. Bildsten, in: W. Lewin, M. van der Klis (Eds.), *Compact Stellar X-Ray Sources*, Cambridge Univ. Press, Cambridge, 2006.
3. A. Parikh, et al., *Prog. Part. Nucl. Phys.* **69**, 225 (2013).
4. S.E. Woosley, R.E. Taam, *Nature* **263**, 101 (1976).
5. P.C. Joss, *Nature* **270**, 301 (1977).
6. B. Lazareff, et al., *Astrophys. J.* **228**, 875 (1979).
7. M. Wiescher, et al., *J. Phys. G: Nucl. Part. Phys.* **25**, R133 (1999).
8. R.K. Wallace, S.E. Woosley, *Astrophys. J. Suppl.* **45**, 389 (1981).
9. H. Schatz, et al., *Phys. Rep.* **294**, 167 (1998).
10. S.E. Woosley, et al., *Astrophys. J. Suppl.* **151**, 75 (2004).
11. H. Schatz, et al., *Phys. Rev. Lett.* **86**, 3471 (2001).
12. V.-V. Elomaa, et al., *Phys. Rev. Lett.* **102**, 252501 (2009).
13. M. Wiescher, et al., *Philos. Trans. R. Soc. London* **356**, 2105 (1998).
14. M. Wang, et al., *Chin. Phys. C* **36**, 1603 (2012).
15. K.I. Hahn, et al., *Phys. Rev. C* **54**, 1999 (1996).

16. S.H. Park, et al., *Phys. Rev. C* **59**, 1182 (1999).
17. S.H. Park, private communications.
18. J. Gómez del Campo, et al., *Phys. Rev. Lett.* **86**, 43 (2001).
19. J.C. Blackmon, et al., *Nucl. Phys. A* **718**, 127c (2003).
20. J.J. He, et al., *Phys. Rev. C* **80**, 042801R (2009).
21. D.W. Bardayan, et al., *Phys. Rev. C* **81**, 065802 (2010).
22. J.J. He, et al., *Eur. Phys. J. A* **47**, 67 (2011).
23. M. Notani, et al., *Nucl. Phys. A* **746**, 113c (2004).
24. J.C. Blackmon, et al., *Nucl. Phys. A* **688**, 142c (2001).
25. B. Harss, et al., *Phys. Rev. Lett.* **82**, 3964 (1999).
26. B. Harss, et al., *Phys. Rev. C* **65**, 035803 (2002).
27. M. Wiescher, et al., *Astrophys. J.* **316**, 162 (1987).
28. J.J. He, et al., *arXive:1001.2053v1*.
29. D.W. Bardayan, et al., *Phys. Rev. C* **85**, 065805 (2012).
30. A.A. Chen, et al., *Phys. Rev. C* **63**, 065807 (2001).
31. J.A. Caggiano, et al., *Phys. Rev. C* **66**, 015804 (2002).
32. G.P.A. Berg, et al., *Nucl. Phys. A* **718**, 608 (2003).
33. A. Matic, et al., *Phys. Rev. C* **80**, 055804 (2009).
34. J. Görres, et al., *Phys. Rev. C* **51**, 392 (1995).
35. J.J. He, et al., *Eur. Phys. J. A* **36**, 1(L) (2008).
36. J.J. He, et al., *Phys. Rev. C* **80**, 015801 (2009).
37. W. Bradfield-Smith, et al., *Phys. Rev. C* **59**, 3402 (1999).
38. D. Groombridge, et al., *Phys. Rev. C* **66**, 055802 (2002).
39. P.J. Salter, et al., *Phys. Rev. Lett.* **108**, 242701 (2012).
40. K.P. Artemov, et al., *Sov. J. Nucl. Phys.* **52**, 408 (1990).
41. W. Galster, et al., *Phys. Rev. C* **44**, 2776 (1991).
42. S. Kubono, *Nucl. Phys. A* **693**, 221 (2001).
43. T. Teranishi, et al., *Phys. Lett. B* **556**, 27 (2003).
44. T. Teranishi, et al., *Phys. Lett. B* **650**, 129 (2007).
45. J.J. He, et al., *Phys. Rev. C* **76**, 055802 (2007).
46. H. Yamaguchi, et al., *Phys. Lett. B* **672**, 230 (2009).
47. Y. Yanagisawa, et al., *Nucl. Instrum. Meth. A* **539**, 74 (2005).
48. S. Kubono, et al., *Eur. Phys. J. A* **13**, 217 (2002).
49. J. Hu, et al., *RIKEN. Accel. Prog. Rep.* **46**, 32 (2013).
50. H. Yamaguchi, et al., *Nucl. Instr. Meth. A* **589**, 150 (2008).
51. J.J. He, et al., *Phys. Rev. C* **88**, 012801R (2013).
52. H. Kumagai, et al., *Nucl. Instr. Meth. A* **470**, 562 (2001).
53. J.F. Ziegler, et al., *The Stopping and Range of Ions in Solids*, Pergamon Press, New York, 1985.
54. A.M. Lane and R.G. Thomas, *Rev. Mod. Phys.* **30**, 257 (1958).
55. P. Descouvemont, *Theoretical Models for Nuclear Astrophysics*, Nova Science Publishers Inc., New York, 2003.
56. C.R. Brune, *Phys. Rev. C* **66**, 044611 (2002).
57. A.St.J. Murphy, et al., *Phys. Rev. C* **79**, 058801 (2009).
58. R.O. Nelson, et al., *Nucl. Instr. Meth. A* **236**, 128 (1985).
59. H.T. Fortune and R. Sherr, *Phys. Rev. Lett.* **84**, 1635 (2000).
60. L.V. Grigorenko, et al., *Phys. Rev. C* **65**, 044612 (2002).
61. D.R. Tilley, et al., *Nucl. Phys. A* **595**, 1 (1995).
62. C. Ruiz, et al., *Phys. Rev. C* **71**, 025802 (2005).
63. T. Rauscher and F.-K. Thielemann, *At. Data Nucl. Data Tables* **75**, 1 (2000).
64. A. Parikh, et al., *Astrophys. J. Suppl.* **178**, 110 (2008).
65. A. Parikh, et al., *Phys. Rev. C* **79**, 045802 (2009).
66. K.Y. Chae, et al., *Phys. Rev. C* **79**, 055804 (2009).